

УДК 539.12.1

MEASUREMENT OF THE TENSOR ANALYZING POWERS IN THE $dd \rightarrow {}^3\text{He}n$ AND $dd \rightarrow {}^3\text{H}p$ REACTIONS AT RIKEN

*V.P.Ladygin*¹, *N.B.Ladygina*¹, *H.Sakai*², *T.Uesaka*³

A new experiment is proposed to measure the angular distribution of the tensor analyzing powers A_{yy} , A_{xx} , and A_{xz} in the $dd \rightarrow {}^3\text{He}n$ and $dd \rightarrow {}^3\text{H}p$ reactions using polarized deuteron beam at RIKEN. These polarization observables are sensitive to the spin-momentum distribution of neutron (proton) in ${}^3\text{He}$ (${}^3\text{H}$) at short distances in the framework of one-nucleon exchange approximation. These measurements will provide new insight into the 3-nucleon system spin structure at distances unreachable at the moment using electromagnetic probes.

The investigation has been performed at the Laboratory of High Energies, JINR.

Измерение тензорных анализирующих способностей в $dd \rightarrow {}^3\text{He}n$ и $dd \rightarrow {}^3\text{H}p$ реакциях в RIKEN

В.П.Ладыгин и др.

Предложен новый эксперимент по измерению углового распределения тензорных анализирующих способностей A_{yy} , A_{xx} и A_{xz} в реакциях $dd \rightarrow {}^3\text{He}n$ и $dd \rightarrow {}^3\text{H}p$ с использованием пучка поляризованных дейтронов RIKEN. Данные поляризационные наблюдаемые чувствительны к импульсному распределению спина нейтрона (протона) в ${}^3\text{He}$ (${}^3\text{H}$) на малых расстояниях в рамках приближения однонуклонного обмена. Эти измерения обеспечат новый взгляд на спиновую структуру 3-нуклонной системы на расстояниях, недостижимых в настоящий момент с использованием электромагнитных пробников.

Работа выполнена в Лаборатории высоких энергий ОИЯИ.

1. PHYSICAL MOTIVATION

1.1. Status of the Study of the ${}^3\text{He}$ Spin Structure. The nonrelativistic Faddeev calculations [1–3] for 3-nucleon bound state predict that the dominant components of the ${}^3\text{He}$ ground state are a symmetric S state, when the ${}^3\text{He}$ spin due to the neutron and two protons are in a spin-singlet state and a D state, when all three nucleons spins are oriented

¹LHE-JINR, 141980 Dubna, Moscow region, Russia

²University of Tokyo, Hongo, Bunkyo, Tokyo 113-0033, Japan

³Saitama University, Saitama 338-8570, Japan

opposite to the ${}^3\text{He}$ spin. The S' component caused by the mixed-symmetry configurations of the nucleons accounts for $\sim 1.5\%$ of the spin-averaged wave function. The S and S' components are found to dominate at zero nucleon momentum, while D state dominates at large momenta.

The momentum distributions of spectator, which are related to the spin-averaged wave function, extracted from inclusive ${}^3\text{He}(e, e')X$ [4] and exclusive ${}^3\text{He}(e, ep)d$ and ${}^3\text{He}(e, ep)pn$ data [5] taking into account final state interaction (FSI) and meson exchange currents (MEC) [6] show a satisfactory agreement with each other except in the region $250 \text{ MeV}/c \leq k \leq 400 \text{ MeV}/c$. The authors mention that the treatment of FSI should be improved both in inclusive and exclusive scattering. The momentum distributions obtained from the exclusive measurements of the ${}^3\text{He}(p, 2p)d$ and ${}^3\text{He}(p, pd)p$ reactions [7] and inclusive measurements of the $A({}^3\text{He}, d)X$ break-up reaction [8], demonstrating a good agreement, show an enhancement of extracted momentum density over calculations performed within relativistic Impulse Approximation (IA) using a Faddeev calculation of the ${}^3\text{He}$ wave function [9] starting from the momentum of spectator in ${}^3\text{He}$ $k > 200 \text{ MeV}/c$. Such a discrepancy can be explained as due to a poor knowledge of the ${}^3\text{He}$ structure at large momenta, as well as to the importance of the reaction mechanisms.

The crucial test of the different approaches in the describing of ${}^3\text{He}$ can be provided by the study of the polarization observables sensitive to the different components of ${}^3\text{He}$. However, the short-range spin structure of ${}^3\text{He}$ has not been investigated so widely as the momentum distributions to date. The ${}^3\vec{\text{He}}(\vec{p}, 2p)$ and ${}^3\vec{\text{He}}(\vec{p}, pn)$ break-up reactions were studied at TRIUMF in quasi-elastic kinematics at 200 [10] and 290 MeV [11] of incident proton energy. In the last experiment, spin observables A_{on} , A_{on} , and A_{nn} were measured up to $q \sim 190$ and $\sim 80 \text{ MeV}/c$ for ${}^3\vec{\text{He}}(\vec{p}, 2p)$ and ${}^3\vec{\text{He}}(\vec{p}, pn)$ reactions, respectively. The results indicate that analyzing powers A_{no} , A_{on} , and A_{nn} are close to the IA calculations for the ${}^3\vec{\text{He}}(\vec{p}, 2p)$ reaction, while for the ${}^3\vec{\text{He}}(\vec{p}, pn)$ there is a strong disagreement with these predictions. The same observables were recently measured at 197 MeV at IUCF Cooler Ring [12] up to $q \sim 400 \text{ MeV}/c$. It was observed that the polarization of the neutron and proton at zero nucleon momentum in ${}^3\text{He}$ are $P_n \sim 0.98$ and $P_p \sim -0.16$, respectively, that is in good agreement with the Faddeev calculations [1–3]. However, at higher momenta there is resemblance, which can be due to the uncertainty of the theoretical calculations, as well as to large rescattering effects.

Polarized electron scattering on polarized ${}^3\text{He}$ target, ${}^3\vec{\text{He}}(\vec{e}, e')X$, also can be used to study the different components of the ${}^3\text{He}$ wave function [1, 2]. However, to describe the experimental results [13] obtained at different relative orientations of electron and ${}^3\text{He}$ spins it is necessary to take into account FSI and MEC in addition to IA, and separation of the ${}^3\text{He}$ structure can be made in the model dependent way. Calculations performed for exclusive ${}^3\vec{\text{He}}(\vec{e}, e')d$ and ${}^3\vec{\text{He}}(\vec{e}, e')pn$ reactions [14] have shown the sensitivity to the various components of the ${}^3\text{He}$ wave function, as well as to FSI and MEC at momenta of spectator above $\sim 250 \text{ MeV}/c$ for these reactions.

Therefore, one can conclude that there are serious theoretical difficulties even in the treatment of the spin-averaged wave function extracted both from electro-disintegration and break-up data. The polarization data are scarce, especially, at high momenta and also are not explained by theory. In this respect, the measurements of new observables sensitive to the short range spin structure of ${}^3\text{He}$ are very desirable.

We propose to measure the tensor analyzing powers of the $dd \rightarrow {}^3\text{He}n$ reaction, which are very sensitive to the neutron spin-momentum distribution in the ${}^3\text{He}$ at short distances [15]. This reaction belongs to the same class of one-nucleon transfer processes as the deuteron-proton backward elastic scattering, $dp \rightarrow pd$ [16], the $d{}^3\text{He} \rightarrow p{}^4\text{He}$ [17] and the $d{}^3\text{He} \rightarrow {}^3\text{He}d$ [18] reactions, extensively studied in the last years. The measurements of the tensor analyzing power T_{20} at a zero degree have shown the sensitivity of this observable to the spin structure of the deuteron [16, 17] and ${}^3\text{He}$ [18], respectively.

1.2. The $dd \rightarrow {}^3\text{He}n$ Reaction in ONE Approximation. Within the framework of one nucleon exchange the $dd \rightarrow {}^3\text{He}n$ process can be described by a sum of 2 diagrams required by the symmetry of the initial state of the reaction. The analysis of the polarization phenomena in the $dd \rightarrow {}^3\text{He}n$ reaction in collinear geometry, when ${}^3\text{He}$ and beam deuteron have the same direction of the momentum in the centre of mass has been performed in Ref. 15. Under these kinematical conditions one of the two diagrams is strongly suppressed (a few orders of magnitude) by the fast decreasing of the deuteron and ${}^3\text{He}$ wave functions versus the relative momenta (at the incident deuteron momenta higher than 200 MeV/c).

The tensor analyzing power $T_{20}(0^\circ)$ due to the polarization of the beam deuteron is simply related to the ${}^3\text{He}$ wave function and can be expressed as [15]

$$T_{20}(0^\circ) = \frac{1}{\sqrt{2}} \frac{2\sqrt{2}uw - w^2}{u^2 + w^2}, \quad (1)$$

where u and w are the S - and D waves of the ${}^3\text{He}$ wave function, respectively.

The expression for $T_{20}(0^\circ)$ agrees with one for the tensor analyzing power T_{20} in the $d{}^3\text{He}$ -backward elastic scattering [18]. However, an undoubted advantage of the investigation of the tensor analyzing power T_{20} in the $dd \rightarrow {}^3\text{He}n$ reaction in comparison with the $d{}^3\text{He}$ -backward elastic scattering is a much higher cross section. The behaviour of the tensor analyzing power $T_{20}(0^\circ)$ in the $dd \rightarrow {}^3\text{He}n$ reaction versus laboratory momentum of the incident deuteron is presented in Fig. 1. The solid, dashed and dotted lines are results of the calculation performed using ${}^3\text{He}$ wave functions from Refs. 9 (with the parametrization of Germond and Wilkin [21]), [22] and [23] (with the parametrization given in Ref. 24), respectively. The relative sign of the S - and D waves of the ${}^3\text{He}$ is taken to be positive according to Ref. 25. One can see high sensitivity of T_{20} behaviour to the used wave functions of the ${}^3\text{He}$ even at relatively low incident momenta. The data on T_{20} in the $d{}^3\text{He}$ -backward elastic scattering obtained at RIKEN [18] are also given by the full symbols in Fig. 1. One can expect at least the same size of effect from D wave in the $dd \rightarrow {}^3\text{He}n$ reaction at a zero degree.

The measurement of the tensor analyzing powers in the $dd \rightarrow {}^3\text{He}n$ reaction at non-zero emission angles provides the probing of higher with respect to 0° relative momenta in the ${}^3\text{He}$. The momentum region up to ~ 600 MeV/c can be probed at 270 MeV at RIKEN.

The angular dependence of the tensor analyzing power A_{yy} in the $dd \rightarrow {}^3\text{He}n$ reaction vs scattering angle of ${}^3\text{He}$ in centre of mass is shown in Figs. 2 *a*), *b*), and *c*) for 140, 200, and 270 MeV, respectively. The solid, dashed and dotted lines are the ONE predictions using ${}^3\text{He}$ wave functions from Refs. 9, 22, and 23, respectively. All calculations have been performed with the use of Paris deuteron wave function [19]. One can see strong sensitivity to the ${}^3\text{He}$ spin structure when ${}^3\text{He}$ is emitted in the forward hemisphere in the centre of mass and strong variation of A_{yy} versus an angle. The dependence of A_{yy} on the used DWF in the vicinity of 90° and larger angles is not significant.

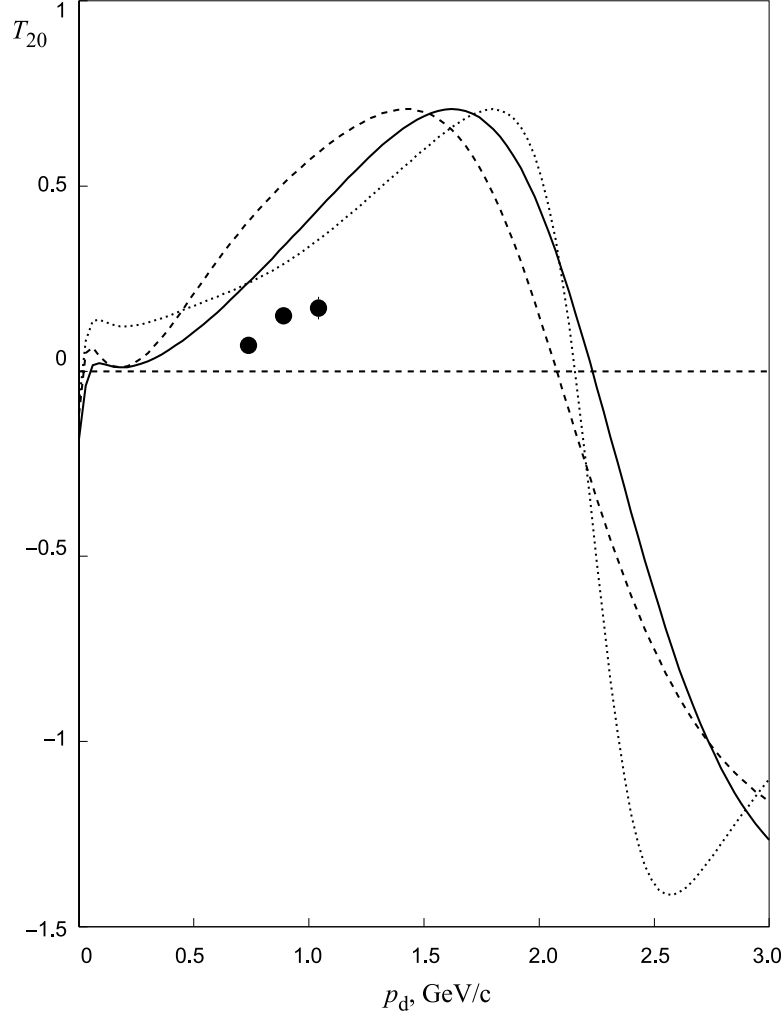


Fig. 1. Tensor analyzing power T_{20} at a zero degree in the $dd \rightarrow {}^3\text{He}n$ reaction. The solid, dashed and dotted lines are the results of ONE calculations with the use of ${}^3\text{He}$ wave functions from Refs. 9, 22, and 23, respectively, and Paris DWF [19]. Symbols are the T_{20} data in the $d^3\text{He} \rightarrow {}^3\text{He}d$ reaction [18]

The behaviours of the tensor analyzing powers A_{xx} (Fig. 3) and A_{xz} (Fig. 4) demonstrate the same features as the behaviour of A_{yy} , namely, strong sensitivity to the ${}^3\text{He}$ spin structure at forward angles and weak dependence on the used deuteron wave function in backward hemisphere. The meaning of the curves are the same as in Fig. 2.

Note, that the vector analyzing power A_y equals zero in ONE approximation. In this respect, its measurement is very desirable to check the validity of the ONE mechanism.

1.3. Study of Charge-Symmetry Breaking. In order to study the possible Charge Symmetry Breaking (CSB), we propose also to measure the tensor analyzing powers in the $dd \rightarrow {}^3\text{He}p$ reaction.

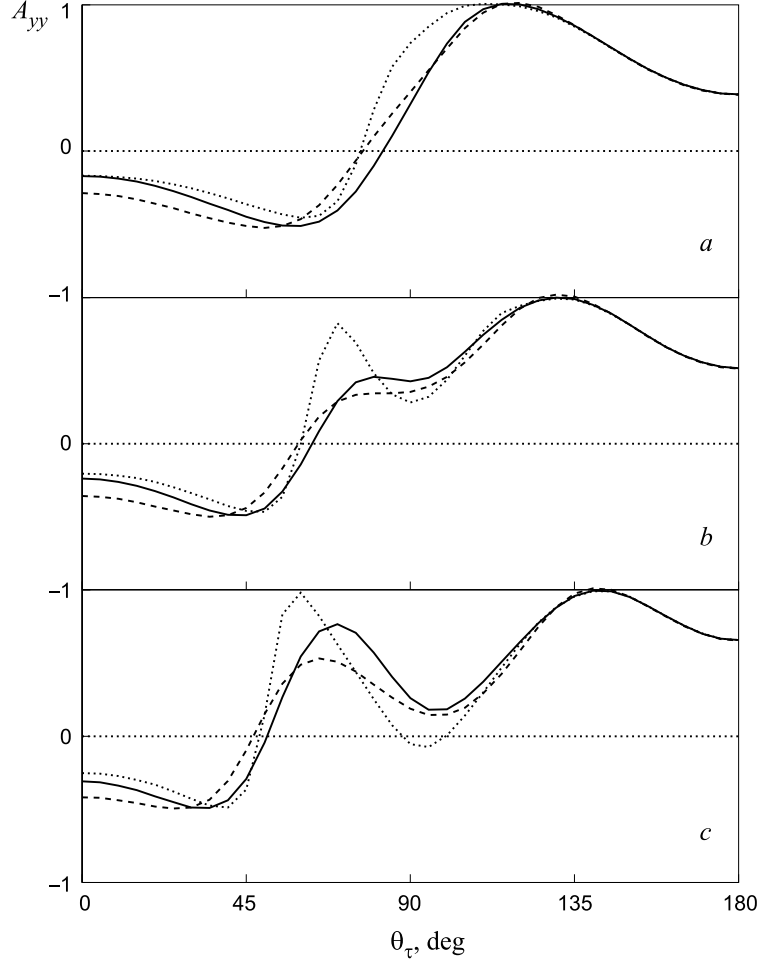


Fig. 2. Tensor analyzing power A_{yy} in the $dd \rightarrow {}^3\text{He}n$ reaction at *a*) 140 MeV, *b*) 200 MeV, and *c*) 270 MeV, respectively. The solid, dashed and dotted lines are the results of ONE calculations with the use of ${}^3\text{He}$ wave functions from Refs. 9, 22, and 23, respectively, and Paris DWF [19]

The CSB in the framework of QCD is related with the difference of the up and down quarks, having slightly different masses, i.e., $m_d - m_u \sim 3$ MeV. The strongest observation of CSB occurs in $\rho^0\omega$ mixing. Their wave functions are given schematically as:

$$\rho^0 = \frac{1}{\sqrt{2}}(|u\bar{u}\rangle - |d\bar{d}\rangle)$$

$$\omega = \frac{1}{\sqrt{2}}(|u\bar{u}\rangle + |d\bar{d}\rangle)$$

so that

$$\langle \rho^0 | H | \omega \rangle = \frac{1}{2} \langle u\bar{u} | H | u\bar{u} \rangle - \frac{1}{2} \langle d\bar{d} | H | d\bar{d} \rangle .$$

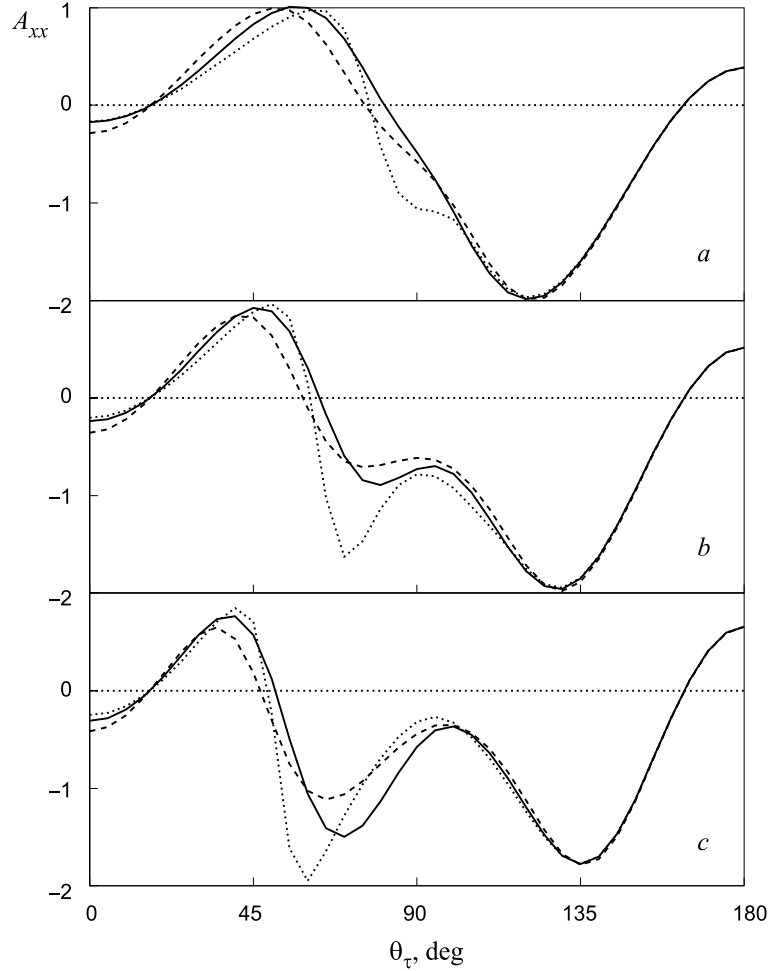


Fig. 3. Tensor analyzing power A_{xx} in the $dd \rightarrow {}^3\text{He}n$ reaction at *a*) 140 MeV, *b*) 200 MeV, and *c*) 270 MeV, respectively. The solid, dashed and dotted lines are the results of ONE calculations with the use of ${}^3\text{He}$ wave functions from Refs. 9, 22, and 23, respectively, and Paris DWF [19]

This term vanishes when $m_u \sim m_d$. The effect of this matrix element is observed in the annihilation $e^+e^- \rightarrow \pi^+\pi^-$ near ρ and ω thresholds [26]. Recent analysis taking into account Coulomb corrections has shown that $\langle \rho^0 | H | \omega \rangle \sim -5100 \text{ MeV}^2$. Apart from this some models predict the strong dependence of $\langle \rho^0 | H | \omega \rangle$ versus q^2 [27]. The crucial review of the current status of CSB study is given in Ref. 28, therefore, we shall discuss the possible CSB only in view of proposed experiment.

Because ${}^3\text{He}$ and ${}^3\text{H}$ are charge-symmetry mirror images, the differences in their observables can be interpreted in terms of CSB. The triton has two np pairs and one nn pair, while ${}^3\text{He}$ has two np pairs and one pp pair, thus CSB in the 3-body system involves the difference between the pp and nn pair potentials. It was found that the scattering length values are -18.5, -23.75, and -17.12 fm of the nn , $np(T=1)$ and pp systems, respectively, (see Ref. 28 and

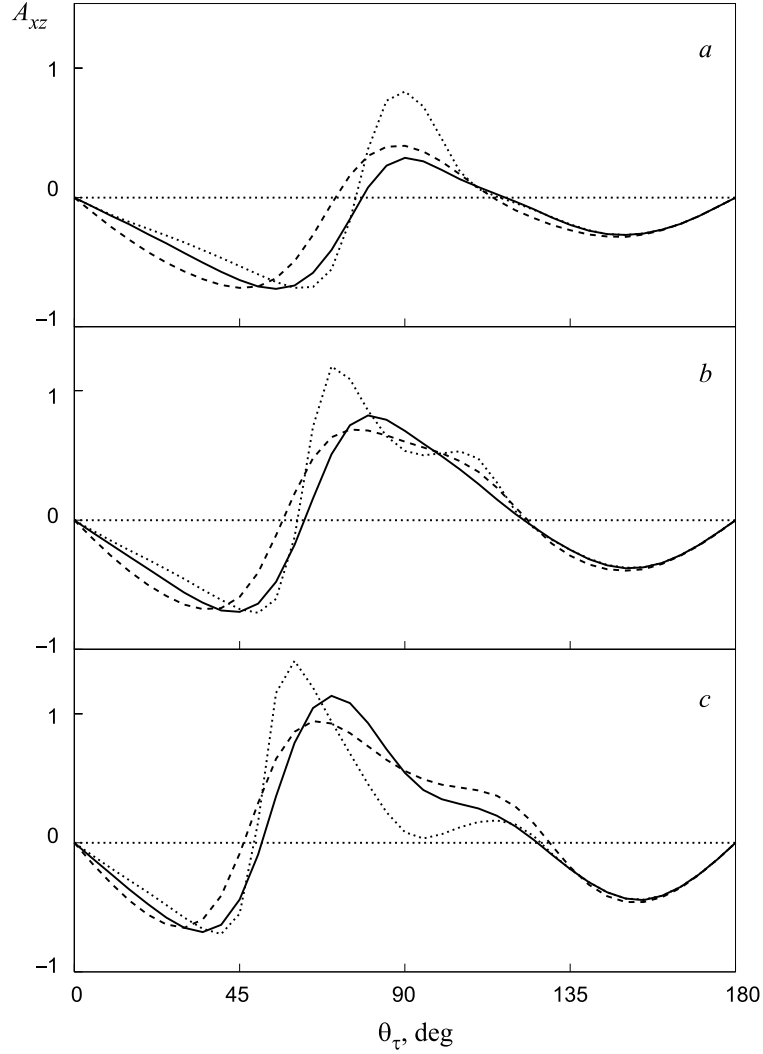


Fig. 4. Tensor analyzing power A_{xz} in the $dd \rightarrow {}^3\text{He}_n$ reaction at *a*) 140 MeV, *b*) 200 MeV, and *c*) 270 MeV, respectively. The solid, dashed and dotted lines are the results of ONE calculations with the use of ${}^3\text{He}$ wave functions from Refs. 9, 22, and 23, respectively, and Paris DWF [19]

corresponding references therein) and can be explained as being caused by the $\rho^0\omega$ mixing.

The traditional three-body bound state calculations, based on the using of the pairwise potentials, fail to reproduce the experimental data for ${}^3\text{H}$ and ${}^3\text{He}$, such as binding energies, charge form factors, *rms* radii, etc. One of the reasons of discrepancy between theoretical and experimental data is the neglect of three-body forces which depend upon the quantum numbers of three nucleons simultaneously [29]. The long-range mechanism for generation of 3-body forces is the 2π exchange, whereas the short-range contribution to 3N force comes from the $\pi\rho$, $\rho\rho$, etc., exchanges.

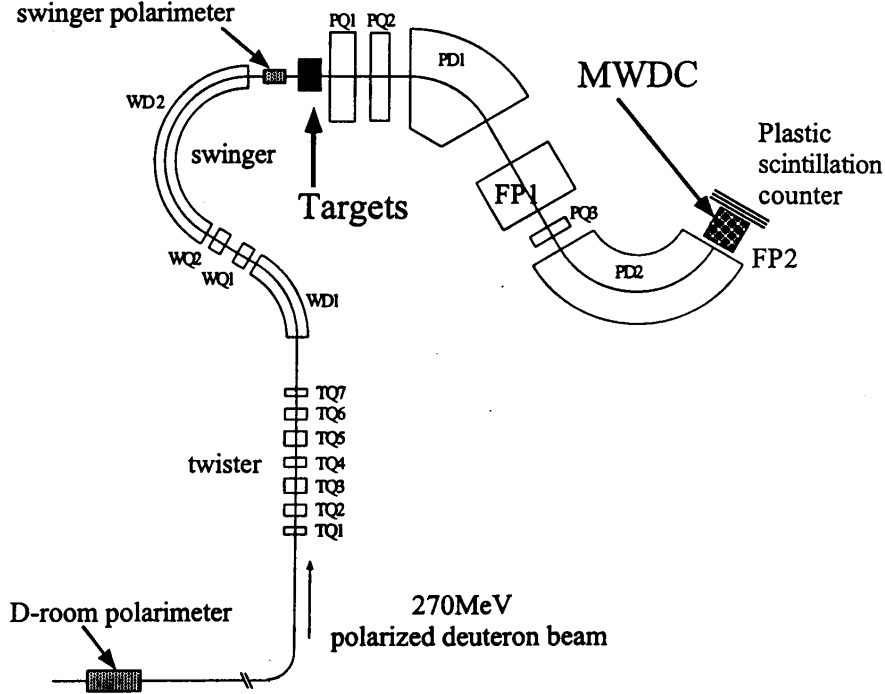


Fig. 5. The layout of SMART spectrograph

The binding-energy difference of triton and ${}^3\text{He}$ is 764 keV and only $693 \pm 19 \pm 5$ keV is due to the electromagnetic contribution [30]. The rest ($\sim 71 \pm 19 \pm 5$ keV) can be explained by the difference in nn and pp scattering lengths, np mass difference, 3-body forces, etc. In this respect the measurement of the tensor analyzing powers, which are not sensitive to the first order Coulomb corrections in comparison with the cross section, in both $dd \rightarrow {}^3\text{He}n$ and $dd \rightarrow {}^3\text{He}p$ reactions, especially, at large angles (large momenta), could provide an additional information on the nature of CSB.

2. EXPERIMENT

We propose to measure the tensor analyzing powers A_{yy} , A_{xx} , and A_{xz} in the $dd \rightarrow {}^3\text{He}n$ reaction using polarized beam of RIKEN [31] up to 270 MeV of the initial deuteron energy. The experiment requires the use of tensor (p_{zz}) and vector (p_z) polarized, as well as unpolarized deuteron beam. The ion source [31] provides a large number of transitions with different tensor and vector polarizations. The chosen combination of the transitions will depend on the measured analyzing power. The measurements of the beam polarization will be done by the use of the beam polarimeter [32] based on the deuteron-proton elastic scattering.

To investigate the $dd \rightarrow {}^3\text{He}n$ (${}^3\text{He}p$) reaction we propose to use SMART (Swinger and Magnetic Analyzer with a Rotator and a Twister) spectrograph, described elsewhere [33,34] and shown in Fig. 5. In this system, the incident beam can be swung by rotating the swinger

magnet, while the magnetic analyzer is fixed. In these experiments the incident beam will be swung from 0° to 40° .

The measurement of ^3He (^3H) momentum and separation from the primary beam will be achieved by the magnetic system of SMART spectrograph consisting of two dipole and three quadrupole magnets ($Q - Q - D - Q - D$). There are two focal planes, FP1 and FP2. The drift chambers placed at the focal plane FP2 will be used as the coordinate detectors. They provide the energy resolution of ~ 300 keV [34]. The solid angle is about 10^{-2} , the angular acceptance in the scattering plane is about 10° .

The identification of the particles will be provided by the measurement of the pulse height and timing information from the trigger plastic-scintillation counters. In the case of the ^3He detection it is necessary to use the information on the charge of the detected particle at the trigger level. It can be easily realized by the changing of the *CFD* thresholds.

The new data acquisition system [35] will be used for the data taking.

The main source of background is the break-up of the deuterons on the target material, since the ^3He from $dd \rightarrow ^3\text{He}n$ has the rigidity close to the rigidity of the proton with a half-momenta of the initial deuteron. The ratio of background protons to ^3He at a zero degree is approximately $10^4 - 10^5$. Fortunately, there is no background from inelastic channels at RIKEN energies. During the experiment we propose to reduce the high voltage on the scintillation counters and drift chambers to suppress the single charged particle rate. The partial suppression of the one-charged particles will be done at the trigger level; the final one, during off-line analysis. In the case of the tritons detection from the $dd \rightarrow ^3\text{H}p$ reaction the selection from background will be provided by the time-of-flight information. One can measure the $dd \rightarrow ^3\text{H}p$ process in the backward hemisphere only, because due to kinematics the tritons have the momentum higher than momenta of the primary beam in the forward hemisphere. Six settings of the angle in the laboratory will allow one to cover the angles of ^3He in the centre of mass from 0° up to 180° due to large angular acceptance of SMART.

The data on the cross section of the $dd \rightarrow ^3\text{He}n$ reaction for the evaluating of the counting rate and beam time request were taken from Ref. 36. The use of the liquid deuterium target of 5 mm in length and intensity of the beam varied between ~ 1 and ~ 100 nA, depending on the detection angle, will provide the error bars of ~ 0.02 for A_{yy} , A_{xx} , and A_{xz} in the step of $\sim 5^\circ$ in the centre of mass. On the other hand, the deuterated polyethylene (CD_2) of ~ 50 mg/cm² thickness also can be used as a target. Such a thickness of the target and a good momentum resolution of SMART will allow one to separate the yield of the studied process from the background from the carbon, and, therefore, it is not necessary to perform the measurements on the carbon target. For instance, the ratio of the background to the useful events was about 6% only in the experiment on the study of the *dp*-backward elastic scattering on the CH_2 target [37].

3. CONCLUSIONS

The behaviour of the tensor analyzing powers A_{yy} , A_{xx} , and A_{xz} in the framework of ONE are completely defined by the ^3He spin structure at the forward angles of ^3He in the centre of mass.

The measurement of these observables at the deuteron initial energy 270 MeV at RIKEN Facility will give the opportunity to investigate the spin structure of ^3He and triton up to the relative momenta of ~ 600 MeV/c for the first time.

The simultaneous measurement of the vector analyzing power A_y is very important to understand the mechanism of the $dd \rightarrow {}^3\text{He}$ reaction.

The measurements of the tensor analyzing powers in the charge-symmetry mirror reactions $dd \rightarrow {}^3\text{He}$ and $dd \rightarrow {}^3\text{H}$ at large angles in the centre of mass, and, hence, short distances, can provide an additional information on the nature of CSB.

Such an experimental programme can be realized for 10 days of RIKEN beam.

4. PERSPECTIVES

First of all, the perspectives are related to the use of the polarized deuteron beam in Dubna.

In Fig. 1 one can see the behaviour of the tensor analyzing power T_{20} in the $dd \rightarrow {}^3\text{He}$ reaction at the incident momenta up to 3 GeV/c. The ONE model predicts the crossing of the zero at the momenta of ~ 2 GeV/c. The continuation of T_{20} measurements in Dubna is very attractive.

At present, the most realizable experiments for this reaction, in addition to the cross section [36] and T_{20} at a zero degree, is the study of the spin correlation C_{yy} defined by the transverse polarization of both initial deuterons [15, 38]. Such investigations could be performed in Dubna using polarized deuteron beam and installed at the Laboratory of High Energies polarized target [39].

The measurement of T_{20} and C_{yy} in future could be a good continuation of the experiment proposed for RIKEN.

Authors are grateful to the Director of LHE of JINR Prof. A.I. Malakhov and the Director of Accelerator Research Facility RIKEN Prof. I. Tanihata for their permanent help. They thank their collaborators S.Afanasiev, K.Hatanaka, M.Hatano, A.Isupov, H.Kato, A.Litvinenko, J.Lukstins, Y.Maeda, J.Nishikawa, H.Okamura, T.Ohinshi, S.Reznikov, N.Sakamoto, S.Sakoda, Y.Satou, K.Sekiguchi, K.Suda, A.Tamii, T.Wakasa, K.Yako and L.Zolin.

References

1. Blankleider B., Woloshyn R.M. — *Phys.Rev.*, 1984, v.C29, p.538.
2. Friar J.L. et al. — *Phys.Rev.*, 1990, v.C42, p.2310.
3. Schulze R.-W., Sauer P.U. — *Phys.Rev.*, 1993, v.C48, p.38.
4. Day D. et al. — *Phys.Rev.Lett.*, 1979, v.43, p.1143;
McCarthy J.S. et al. — *Phys.Rev.*, 1976, v.C13, p.712.
5. Jans E. et al. — *Phys.Rev.Lett.*, 1982, v.49, p.974;
Jans E. et al. — *Nucl.Phys.*, 1987, v.A475, p.687.
6. Ciofi degli Atti C., Pace E., Salme G. — *Phys.Rev.*, 1989, v.C39, p.259; *Phys.Rev.*, 1991, v.C43, p.1155.
7. Epstein M.B. et al. — *Phys.Rev.*, 1985, v.C32, p.967;
Kitching P. et al. — *Phys.Rev.*, 1972, v.C6, p.769.

8. Ableev V.G. et al. — *JETP Lett.*, 1987, v.45, p.596.
9. Schiavilla R., Pandharipande V.R., Wiringa R.B. — *Nucl.Phys.*, 1986, v.A449, p.219.
10. Brash E.J. et al. — *Phys.Rev.*, 1993, v.C47, p.2064.
11. Rahav A. et al. — *Phys.Lett.*, 1992, v.B275, p.259;
Rahav A. et al. — *Phys.Rev.*, 1992, v.C46, p.1167.
12. Miller M.A. et al. — *Phys.Rev.Lett.*, 1995, v.74, p.502.
13. Woodward C.E. et al. — *Phys.Rev.Lett.*, 1990, v.65, p.698;
Jones-Woodward C.E. et al. — *Phys.Rev.*, 1991, v.C44, p.R571;
Thompson A.K. et al. — *Phys.Rev.Lett.*, 1992, v.68, p.2901;
Meyerhoff M. et.al. — *Phys.Lett.*, 1994, v.B327, p.201.
14. Laget J.M. — *Phys.Lett.*, 1992, v.B276, p.398.
15. Ladygin V.P., Ladygina N.B. — *Phys.Atom.Nucl.*, 1996, v.59, p.89;
Ladygin V.P., Ladygina N.B. — *Nuovo Cim.*, 1999, v.A112, p.855.
16. Punjabi V. et al. — *Phys.Lett.*, 1995, v.B350, p.178;
Azhgirey L.S. et al. — *Phys.Lett.*, 1997, B391, p.22.
17. Uesaka T. et al. — *Phys.Lett.*, 1999, v.B467, p.199.
Uesaka T. et al. — In: *Proc. of APFB99, Noda/Kashiwa, August 1999.*
18. Tanifuji M. et al. — *Phys.Rev.*, 2000, v.C61, p.024602.
19. Lacombe M. et al. — *Phys.Lett.*, 1981, v.B101, p.139.
20. Machleidt R. et al. — *Phys.Rep.*, 1987, v.149, p.1.
21. Germond J.-F., Wilkin C. — *J.Phys.G: Nucl.Phys.*, 1988, v.14, p.181.
22. Laget J.M., Lecolley J.F., Lefebvres F. — *Nucl.Phys.*, 1981, v.A370, p.479.
23. Santos F.D., Eiro A.M., Barosso A. — *Phys.Rev.*, 1979, v.C19, p.238.
24. Uzikov Yu.N. — *EChAYa*, 1998, v.29, p.1010.
25. Eiro A.M., Santos F.D. — *J.Phys.G: Nucl.Phys.*, 1990, v.16, p.139.
26. Quenzer A. et al. — *Phys.Lett.*, 1978, v.B76, p.512;
Barkov L.M. et al. — *Nucl.Phys.*, 1985, v.A256, p.365.
27. Krein G., Thomas A.W., Williams A.G. — *Phys.Lett.*, 1993, v.B317, p.293.
28. Miller G.A., Nefkens B.M.K., Slaus I. — *Phys.Rep.*, 1990, v.194, p.1.
29. Coon S.A. et al. — *Nucl.Phys.*, 1979, v.A317, p.242;
Coon S.A., Glöckle W. — *Phys.Rev.*, 1981, v.C23, p.1790.

30. Coon S.A., Barrett R.C. — *Phys. Rev.*, 1987, v.C36, p.2189;
Friar J.L., Gibson B.F., Payne G.L. — *Phys.Rev.*, 1987, v.C36, p.1140.
31. Okamura H. et al. — *AIP Conf.Proc.*, 1993, v.293, p.84.
32. Sakamoto N. et al. — *Phys.Lett.*, 1996, v.367, p.60.
33. Ichihara T. et al. — *Nucl.Phys.*, 1994, v.A569, p.287c.
34. Ohnishi T. — Master Thesis, unpublished.
35. Okamura H. — *RIKEN Accel.Prog.Rep.*, 1999, v.32, p.159; *Nucl.Instr. and Meth.*, 2000, v.A443, p.194.
36. Roy M. et al. — *Phys.Lett.*, 1969, v.B29, p.95;
Bizard G. et al. — *Phys.Rev.*, 1980, v.C22, p.1632.
37. Sekiguchi K. et al. — In: *Proc. of APFB99, Noda/Kashiwa, August 1999*;
Sekiguchi K., private communication.
38. Ladygin V.P., Ladygina N.B. — *JINR Rapid.Comm.*, 1995, 4[72]-95, p.19.
39. Lehar F. et al. — *Nucl.Instr.and Meth.*, 1995, v.A356, p.58.

Received on April 27, 2000.